DENSE NONAQUEOUS PHASE LIQUID MIGRATION IN A COMPLEX MULTI-AQUIFER SYSTEM

D.B. Stephens, M. Piepho, J.A. Kelsey, M.A. Prieksat, and M.D. Ankeny, Daniel B. Stephens & Associates, Inc., 6020 Academy Road NE, Suite 100, Albuquerque, NM, 87109

ABSTRACT A laboratory experiment was conducted to demonstrate the behavior of dense nonaqueous phase liquid (DNAPL) 1,1,1-trichloroethane (TCA) in a complex aquifer system. The system simulated consists of two unconfined aquifers separated by a low permeable bedrock perching layer that contains a fracture. In contrast to previous work by other researchers of DNAPL migration in hydrostatic conditions, in this experiment, prior to and during the DNAPL release, ground water flow occurs from the upper to lower aquifer via the fracture. Although the experiment illustrates that DNAPL may migrate rapidly in narrow pathways, the observations were predicted rather well by a simplified analytical solution and a numerical simulation with the multi-phase flow and transport code TOUGH-2. With recharge to the lower aquifer occurring through the fracture, a DNAPL pool did not develop prior to its entry into the fracture.

KEYWORDS: nonaqueous phase liquids, transport modeling

INTRODUCTION

Understanding and predicting the migration of DNAPL through the subsurface is important in many ground water transport investigations. For example, in some instances, it is essential to reconstruct this process in order to predict the nature and timing of the release for insurance coverage cases. Frequently, DNAPL migration is at the heart of litigation or allocation proceedings over remedial costs between responsible parties.

Over the last decade or so, mathematical tools have been developed to facilitate analyzing DNAPL migration, as summarized by Cohen and Mercer [1] and Pankow and Cherry [2]. For instance, analytical solutions have been proposed to assess the maximum thickness of a stable DNAPL pool in the vadose zone and the thickness of the DNAPL pool required to penetrate the capillary fringe, as well as solutions to evaluate the DNAPL pool height necessary to penetrate a water-filled fracture in an aquitard. Most analytical solutions for DNAPL migration in aquifers pertain to hydrostatic conditions in which the hydraulic head gradient is zero. However, Kueper and McWhorter [3] used numerical simulations to address the DNAPL travel time across a fractured aquitard separating two aquifers, with upward or downward flow in the fracture and fully-saturated conditions below the aquitard.

In many hydrogeologic environments, one is likely to encounter perched ground water, that is, a relatively permeable, water saturated media of limited areal extent bounded below by a low permeable layer that is separated from the underlying regional water table by an unsaturated zone. Perched aquifers usually develop where the downward percolation rate through the vadose zone is greater than the water-saturated hydraulic conductivity of an impeding layer. Especially in humid climates, there can be significant downward flux from the perched aquifers and through the low permeable perching beds which becomes recharge to the underlying regional

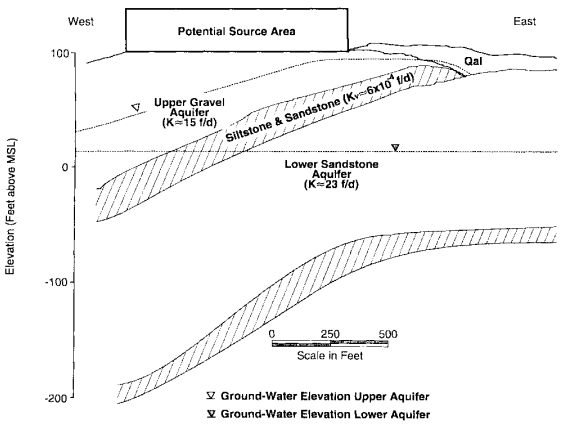

FIGURE 1. GEOLOGICAL CROSS-SECTION.

aquifer. Continuous fractures or connected fracture networks in the perching layers comprise preferential pathways for both the recharge and downward DNAPL migration.

In this article, we present a new analytical solution for the problem of vertical DNAPL migration through fractures that terminate in unsaturated porous media. In contrast to prior work which pertains primarily to fully saturated media and hydrostatic conditions, the new solution recognizes the contribution of natural ground water recharge through the vadose zone. In this article, we also demonstrate the behavior of DNAPL migration through a fractured perching layer using a sandbox experiment and compare predictions from the new analytical solution to experimental observations of travel time across the fracture. In a companion paper, we present the results of a multiphase flow simulation of the laboratory sandbox experiment.

The analyses presented in this article were developed in support of litigation between two adjacent industrial facilities seeking to allocate costs for remediation of chlorinated hydrocarbon in ground water.

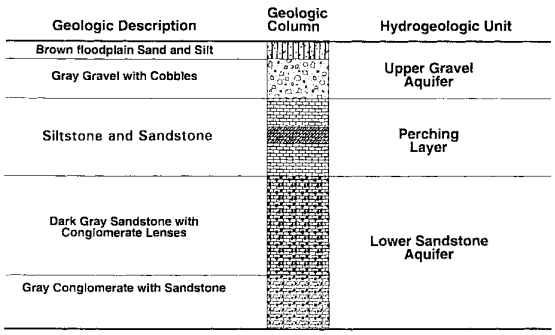

FIGURE 2. STRATIGRAPHIC UNITS.

HYDROGEOLOGIC SETTING AND LITIGATION ISSUES

The site that provided motivation for this analysis is located in the Pacific Northwest where mean annual precipitation is about 94 cm/yr (37 inches per year). The site is situated on a gentle hillside sloping northward toward the floodplain of the Columbia River. The site is underlain by two bedrock aquifers which are separated by a fractured perching layer; both the upper aquifer and the perching layer dip westward at about 5 degrees (Figure 1). The upper unconfined aquifer is predominantly sandstone and conglomerate that is perched on a low-permeable sequence comprised mostly of sandstone and siltstone (Figure 2). The lower aquifer is an unconfined sandstone aquifer which has a water table located a few meters below the base of the siltstone perching layer in the area of interest. Thus, there is an unsaturated zone below the siltstone. The difference in head across the siltstone, as well as the slickensides, fractures, and joints observed in some drill cores and in shallow excavations in the perching unit, indicate that there is potential for downward ground water flow from the upper to the lower aquifer. Although field investigations did not attempt to quantify fracture aperture or connectivity, a literature review indicated

that fracture apertures of 10 to more than 100 microns would not be unexpected in siltstone.

The upper aquifer contains volatile organic chemicals, primarily solvents such as 1,1,1-TCA and trichloroethylene (TCE), that are believed to have migrated as a DNAPL phase. An issue in the litigation was the potential for a DNAPL to migrate downward through fractures across the siltstone perching layer, through the lower vadose zone, and into the lower aquifer.

One party argued that all fractures in the perching unit were discontinuous and filled. This party calculated vertical travel time across the perching unit using Darcy's equation and the assumption of vertical porous media flow through each subunit of the perching layer. The effective hydraulic conductivity was based on a thickness-weighted harmonic mean of laboratory tests of core samples collected from the four subunits. Using the mean hydraulic conductivity of 5.9×10^{-4} feet per day, vertical gradient of 1.4, and effective porosity of 0.25, the predicted travel time across the perching layer was about 40 years, based on porous media flow. This party further argued, based on a hydrostatic analysis, that a critical DNAPL pool height of several centimeters to perhaps more than a meter would be required before migration of DNAPL through the fractured perching layer could occur. Thus, a considerable volume of solvent could be "stored" in the vadose zone and upper aquifer before DNAPL could migrate across the aquitard. Based on the long calculated travel time and DNAPL storage potential above the perching layer, this party argued that any DNAPL constituents in the lower aquifer were derived from either an off-site source or from improperly constructed but recently plugged production wells in which contaminants migrated from the upper aquifer to impact only a localized part of the lower aquifer.

The other party argued that vertically continuous, open fractures probably do occur at the site, and that relatively rapid DNAPL transport from the shallow to the deep aquifer is facilitated by fractures in the low-permeable perching layer which also transmit ground water as recharge naturally to the lower aquifer. The potential for DNAPL migration across the aquitard is important, not only to allocation of costs to remediate the contamination currently present in the lower aquifer, but to assessing the long-term effectiveness of a remedy for the lower aquifer that could be prolonged by continuous leakage of contaminants across the perching layer.

MATHEMATICAL MODEL DEVELOPMENT

The aquifer and fractured perching layer system described above is conceptualized as shown in Figure 3 for purposes of mathematical model development. We assume that there is a constant height of water, h_w, above a NAPL-water pool mixture, and the DNAPL water pool has constant thickness, h_{nw}, above the base of this aquifer. The DNAPL water pool consists of both water and DNAPL, with the percentage of pore space occupied by DNAPL, $\%S_n$, increasing toward the base of the fracture (e.g., [3]). In the general case, we assume that the fracture will also contain both water and DNAPL. Inasmuch as the porous media below the perched layer is unsaturated, the fluid pressure is assumed to be atmospheric below the fracture. In our mathematical analysis, we neglect DNAPL entry pressures and capillary pressure between the various fluid phases; these effects are considered in the companion

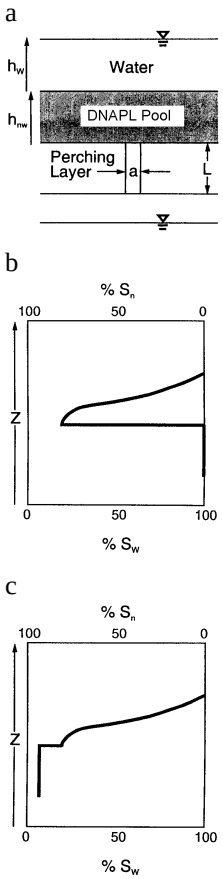

FIGURE 3. (a) SCHEMATIC DIAGRAM OF DNAPL POOL ABOVE A FRACTURED PERCHING LAYER; (b) FLUID SATURATION PROFILE AT INCIPIENT PENETRATION OF DNAPL; AND (c) FLUID SATURATION PROFILE AFTER DNAPL ENTRY INTO FRACTURE.

article where we evaluate the process through a multiphase flow simulation. We also ignore the potential for DNAPL to absorb into the porous matrix as it migrates through the fracture.

The travel time for DNAPL to migrate through the fracture is determined from the calculated hydraulic gradient, intrinsic permeability, and effective saturation of DNAPL above and in the fracture. We assume there is a single, vertical fracture through the siltstone perching layer. The hydraulic gradient is

$$\bar{i}_n = \frac{h_w \rho_w + (\bar{S}_{nh}\rho_n + \bar{S}_{wh}\rho_w) h_{nw} + (\bar{S}_{nL}\rho_n + \bar{S}_{wL}\rho_w) L}{\rho_n L}, \quad (1)$$

where L = the fracture length, ρ_n = DNAPL density, ρ_w = water density, $\bar{S}_{nh}$ = average saturation of DNAPL in the mixed DNAPL water pool above the fracture, $\bar{S}_{wh}$ = average saturation of water in the mixed DNAPL water pool above the fracture, $\bar{S}_{nL}$ = average saturation of DNAPL within the fracture, $\bar{S}_{wL}$ = average saturation of water within the fracture, and h_w = height of pure water pool above the mixed DNAPL water pool.

The DNAPL pore velocity in the fracture is

$$V_{pn} = \frac{\rho_n g k^f k_{rn}}{\mu_n n^f \bar{S}_{nL}} \bar{i}_n, \quad (2)$$

where $k_{r\,n}$ = relative permeability of NAPL in the fracture, k^f = intrinsic permeability of the fracture, n^f = porosity of the fracture, μ_n = dynamic viscosity of DNAPL, and g = gravitational constant (9.8 m/s^2).

Where the fracture is a smooth plane having a constant aperture, a, the intrinsic permeability is $a^2/12$. In such a case, the DNAPL travel time through the smooth fracture, L/V_{pn}, is

$$t_n = \frac{12 \mu_n \bar{S}_{nL} L^2}{a^2 g k_{rn} [\rho_w h_w + (\bar{S}_{nh}\rho_n + \bar{S}_{wh}\rho_w) h_{nw} + (\bar{S}_{nL}\rho_n + \bar{S}_{wL}\rho_w) L]}. \quad (3)$$

If we assume that the DNAPL water pool above the fracture is infinitesimally thin and the fracture only contains DNAPL, the travel time through the fracture is simply

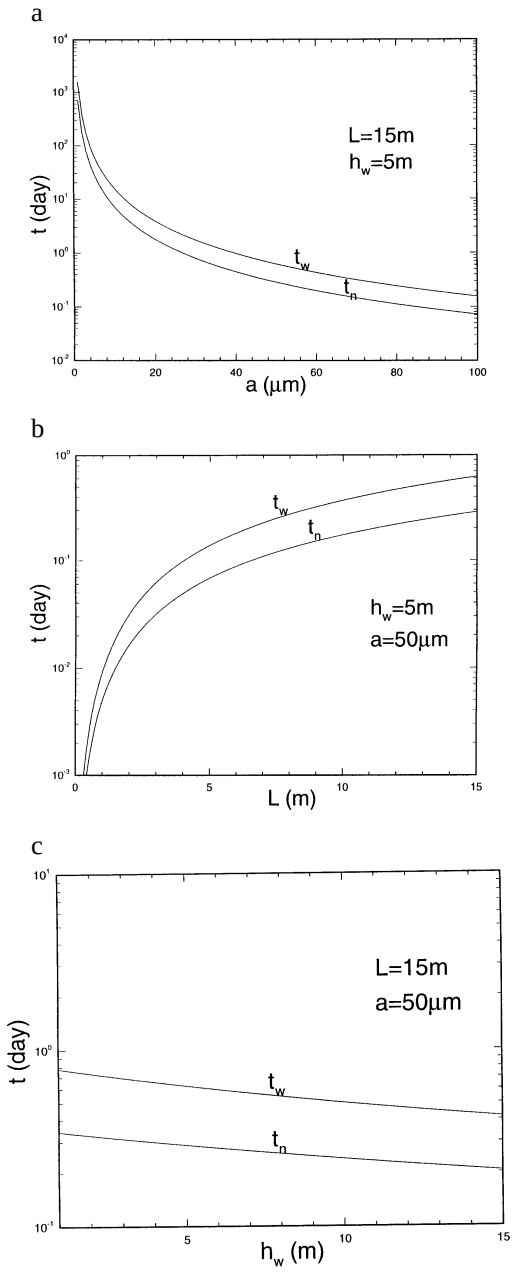

FIGURE 4. PREDICTED DNAPL AND WATER TRAVEL TIMES AS A FUNCTION OF (a) FRACTURE APERTURE, (b) FRACTURE LENGTH, AND (c) HEAD OF WATER ABOVE FRACTIONS.

$$t_n = \frac{12\mu_n L^2}{a^2 g\,[\rho_w h_w + \rho_n L]}\ . \qquad (4)$$

Note that in this simplification, $h_{nw} = 0$, $\overline{S}_{nL} = 1$, $\overline{S}_{wL} = 0$, $n^f = 1$,, and $k_{rn} = 1$.

For cases of water only, the water pore velocity is

$$V_{pw} = \frac{\rho_w g\, a^2\, (h_w + L)}{12\mu_w L} \qquad (5)$$

and the travel time for water in the fracture becomes

$$t_w = \frac{L}{V_{pw}} = \frac{12\mu_w L^2}{\rho_w g(h_w + L)a^2}\,. \qquad (6)$$

To illustrate the behavior of Equations 4 and 6, we map the dependence of travel time on fracture aperture for water and DNAPL to cross a 15 meter (m) thick perching layer (Figure 4a). In Figure 4b, we show the dependence of travel time on fracture length for a 50 micron fracture aperture, and Figure 4c illustrates the effect of saturated thickness in the upper aquifer on travel times in the fracture.

LABORATORY EXPERIMENT

The purpose of the laboratory experiment is 1) to visualize the transport of DNAPL through a fractured perching layer and 2) to assess the travel time for purposes of validating the approximate mathematical model. The experimental parameters were selected to capture the critical physical elements of the hydrogeologic setting of the site which was the subject of the litigation.

The tank was constructed from 0.95 cm thick non-tempered glass (Figure 5). The upper section of the tank was 114.3 cm long by 29.2 cm wide by 1.1 cm thick; this section was analogous to the upper gravel aquifer and was filled with 10/20 silica sand with an effective grain size (d_{10}) of 0.97 mm and a saturated hydraulic conductivity of 7.7 x 10^{-2} cm/s. The lower part of the tank was 58.4 cm long by 29.2 cm wide by 1.1 cm thick. This section of the tank represented the finer-textured lower sandstone aquifer

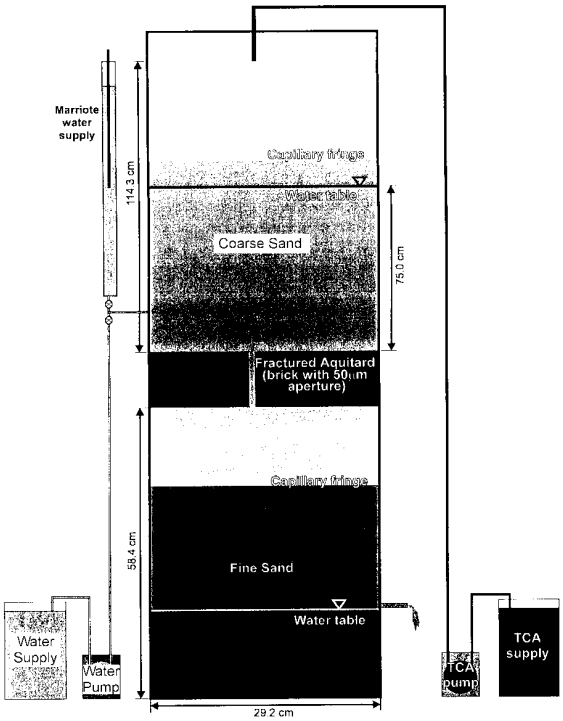

FIGURE 5. LABORATORY EXPERIMENTAL SET-UP FOR DNAPL MIGRATION.

and was filled with a commercial glass bead abrasive with a d_{10} value of 0.19 mm and saturated hydraulic conductivity of 2.9×10^{-2} cm/s. Water retention curves for each of the porous materials are shown in Figure 6. All sand was placed in the tank by pouring it dry.

To create the fractured perching layer analogue, we separated the upper and lower sections of the tank by two red bricks (Figure 5). A 51 micron aperture was created between the brick ends by annealing them to a sandwich of two 0.32 cm thick glass plates that were glued together with two 51 micron feeler gauges inserted between the two glass plates. When the adhesive dried, the feeler gauges were removed to create the opening. Together, the two bricks and the glass plates were 29.2 cm wide by 9.2 cm long, vertically, by 5.8 cm thick.

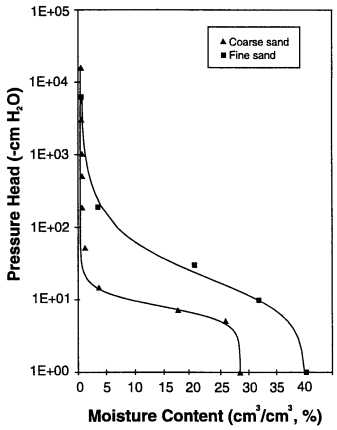

FIGURE 6. SOIL-WATER CHARACTERISTIC CURVES FOR SANDS IN THE LABORATORY EXPERIMENT.

A steady state water flow of 1.8 ml/min was applied by pumping water into the upper section while the water table above the fracture was kept constant at a height of 75 cm above the brick by a marriote apparatus (Figure 5). The water level in the lower section of the tank was kept constant by inserting an overflow tube into the side of the sand tank. The vadose zone above the lower aquifer was vented to the atmosphere. The height of the capillary fringe in the fine sand comprising the lower aquifer was approximately 28 cm above the water table, based upon visual inspection. The downward hydraulic head gradient across the fracture was about 9.15 cm/cm.

1,1,1-TCA, dyed with D & C RED 17, was selected as the DNAPL. According to the distributor, the TCA specific gravity is 1.319 at 25ºC, and dynamic viscosity is 0.86 cP at 20ºC. The TCA was pumped through a 0.16 cm diameter norprene tube to the top of the sand tank at a rate of 5.0 ml/min (1.9 gal/d; 12 bbls/yr) at a temperature of 20.4ºC. Video and still photography documented the migration behavior of the DNAPL.

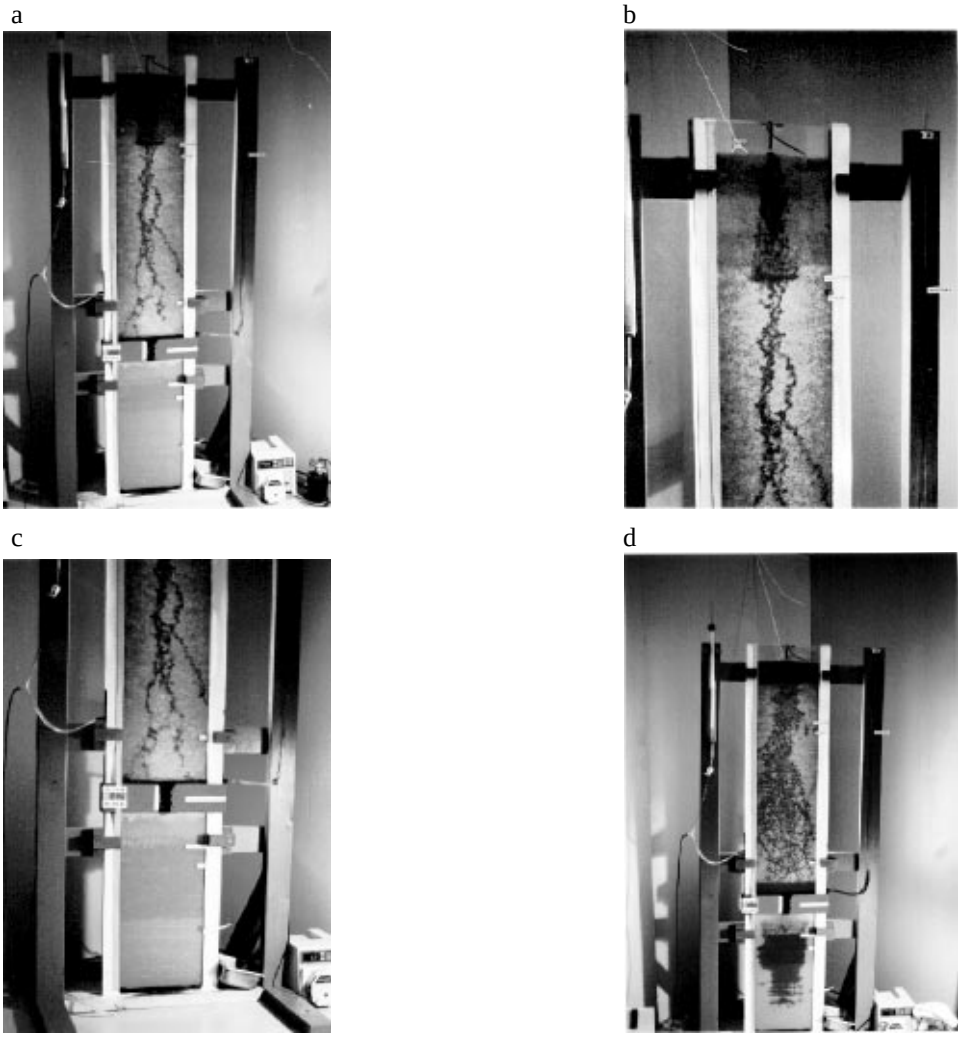

FIGURE 7. TCA MIGRATION AFTER (a) 12:53 MINUTES, (b) 13:29 MINUTES, SHOWING DNAPL ON CAPILLARY FRINGE, (c) AFTER 14:25 MINUTES, SHOWING DNAPL EXITING THE FRACTURE, AND (d) AFTER 22:01 MINUTES.

RESULTS AND DISCUSSION

The predicted travel time for TCA migration through the fracture was calculated using Equation 4 and physical properties presented earlier in the text. The predicted travel time is about 4 seconds.

The TCA migration in the early stage of the flow visualization experiment is shown in Figure 7a. In the upper vadose zone, the TCA tends to spread laterally rather gradually as it migrates downward primarily through air-filled pores [4]. Note, as the TCA reached the capillary fringe, that the TCA tends to pool slightly before it migrates to the water table. This is because the capillary pressure at the base of the DNAPL pool must exceed the DNAPL displacement pressure (a characteristic of the porous media and water-DNAPL interfacial tension) before it can displace the water and migrate deeper.

For comparison of the experimental results with the hydrostatic analysis, the theoretical

height of the TCA pool, Z_n, required to penetrate the capillary fringe was calculated from Equation 5-16 in Cohen and Mercer [1]:

$$Z_n = \frac{2\sigma_{DW} \cos \alpha}{rg\rho_n}, \quad (7)$$

where σ_{DW} = interfacial tension between TCA and water (45 dynes/cm), α = contact angle (assume zero), r = mean pore radius (cm), g = gravity constant (980 cm/s^2), and ρ_n = TCA density (1.339 g/cm^3 at 20ºC).

The mean pore radius is one source of uncertainty in Equation 7. Dullien [5] indicates mean pore diameter is as much as 40% of the mean particle diameter (r = 0.4 $d_{50}/2$ = 0.28 mm). Hubbert [6] reports that the mean pore radius is one-eighth of the mean pore diameter (r = $d_{50}/8$ = 0.17 mm). Holtz and Kovacs [7] suggest that the mean pore radius is one-tenth of the ten percent finer particle size (r = 0.1 d_{10} = 0.097 mm). Thus, the mean pore radius "r" is calculated as r = 0.4$d_{50}/2$ = .28 mm. The mean pore radius could also be calculated from the capillary rise equation:

$$r = \frac{2\sigma \cos\alpha}{\rho g\ h_c}, \quad (8)$$

where h_c is obtained from the moisture retention curve ($h_c \approx 10$ cm); in this case r = 0.15 mm which agrees well with Hubbert's equation. From this range of values for r substituted into Equation 7, the TCA DNAPL pool height should range from 2.4 to 7.1 cm under hydrostatic conditions. The observed thickness of the TCA pool on the capillary fringe was minimal (unmeasurable) immediately prior to the time it penetrated the capillary fringe. Subsequently, the maximum DNAPL thickness observed on the capillary fringe was about 1 cm by visual inspection. Thus, the hydrostatic analysis overestimates storage in the vadose zone above the capillary fringe for this flow system.

Figure 7b illustrates that below the capillary fringe, the DNAPL migrates through only a small portion of the initially water-saturated zone, following a narrow, elongated, and tortuous path. The pattern is attributable to instability between the fluids, where the more dense fluid, TCA, is displacing water. Heterogeneity in pore size also leads to DNAPL migration preferentially through the largest diameter pores. The TCA reached the left side of the perching layer approximately 12 minutes and 53 seconds after the release (Figure 7a), and migrated laterally to the fracture at about 13 minutes 29 seconds. By about 14 minutes, the TCA was clearly observed in the lower vadose zone below the brick (Figure 7c). Thus, the visual data indicate that the travel time through the fracture was approximately 30 seconds. It is likely that the actual travel time for the first particles to arrive was considerably shorter, because the initial mass would not be sufficient to be detected visually.

We compare the experimental results showing the thickness of DNAPL, H_D, required to displace water from the fracture with a solution for the hydrostatic case [3]:

$$H_D = \frac{2\sigma_{DW}}{\Delta\rho ge} - \frac{P_D}{\Delta\rho g}, \quad (9)$$

where σ_{DW} = interfacial tension between TCA and water (45 dynes/cm), $\Delta\rho$ = density difference between TCA and water (0.341 g/cm^3 at 20ºC), g = gravity (980 cm/s^2), e = fracture aperture (0.0051 cm), and P_D = displacement pressure (6,125 dynes/cm^2).

According to Kueper and McWhorter [3], P_D is negligible for coarse-grained material. In our study, however, the displacement

pressure, P_D, for DNAPL to displace water in the coarse sand was estimated from the air-entry value, ψ_a, on the soil-water characteristic curve (Figure 6):

$$P_D = \left(\frac{\sigma_{DW}}{\sigma_{WA}}\right)\psi_a \rho_w g = 6125 \ \frac{dynes}{cm^2}, \qquad (10)$$

where σ_{DW} = 45 dynes/cm, σ_{WA} = 72 dynes/cm, and ψ_a = ~10 cm.

In theory, Equation 9 predicts that DNAPL would have to pool to a thickness, H_D, of about 34 cm before it entered the fracture. By contrast, in the experiment with downward water flow occurring at the time DNAPL arrived at the fracture, TCA migrated across the fracture without any appreciable pool formation.

The late stage behavior is illustrated in Figure 7d. In the upper aquifer, the TCA paths have spread laterally and have filled more of the available pore space. Note that a significant DNAPL pool eventually formed above the fracture. Below the fracture, in the finer textured vadose zone and aquifer, the predominant DNAPL pathway is vertically downward and appears to be well contained within the walls of the sand box.

APPLICATION

The new analytical solution (Equation 4) was applied to the field site in the Pacific Northwest to calculate the DNAPL travel time across the perching layer, for the situation depicted in Figure 1 and as simplified in Figure 3a. We assume there is a single, smooth, vertical fracture 14.6 m long and 50 microns wide that completely penetrated the perching layer. Applying Equation 4, the travel time through the perching layer is only 43 minutes. This is considerably faster than the 40-year travel time calculated by the party who based their travel time calculations on Darcy's equation and a harmonic mean hydraulic conductivity computed from laboratory measurements on core samples. The mathematical model and laboratory experiment support the argument that, at the field site, contamination in the lower aquifer could be attributed to downward migration from the upper aquifer. A court ruling on the allocation of cleanup costs in the lower aquifer recognized transport across the fractured aquitard in reaching its decision.

CONCLUSIONS

A new simple analytical solution for DNAPL transport in a fracture has been derived and successfully tested in a laboratory sand box experiment. There was no significant delay in DNAPL penetration into the fracture for the dynamic flow field and conditions of the experiment. This is in contrast with the behavior expected in a hydrostatic flow field. There was no evidence that a DNAPL pool formed prior to transport of DNAPL into the fracture. Therefore, it is reasonable to neglect this aspect in computing DNAPL travel times from porous through fractured media for similar field conditions.

The approximate analytical solution underestimates the travel time through the fracture which we determined by visual detection of the dyed TCA. Visual detection, however, may not be sufficiently accurate to test the validity of the solution. Further evaluation of the approximate solution is the subject of the companion article.

The DNAPL release rate used in this experiment (1.9 gallons/day) is not unlike what might be expected to cause very large dissolved phase contaminant plumes in aquifers. The experiment suggests that the vadose zone pathways are likely to be predominantly vertical, at least in

homogeneous media. For this release scenario in the laboratory experiment, the visual pathways in both the upper and lower sections of porous media indicate that samples of soil matrix from vertical cores would be unlikely to detect the DNAPL unless the boring were directly below the source. One implication is that deep soil gas measurements which sample a relatively large volume of soil may be a preferable means to evaluate contaminant transport pathways through the vadose zone.

ACKNOWLEDGMENT

The authors want to thank Cascade Corporation for the opportunity to undertake this research. The technical collaboration with Ms. Dorothy Atwood and her staff at Emcon, Inc., Portland, Oregon, is very much appreciated. And, we are also grateful to Mr. George W. McKallip, Jr., of Kennedy, King, and Zimmer, Portland, Oregon for assisting in developing experimental objectives and facilitating the completion of the project.

REFERENCES

1. R.M. Cohen and J.W. Mercer, DNAPL Site Evaluation, C.K. Smolley, Boca Raton, Florida, 1993.

2. J.F. Pankow and J.A. Cherry, Dense Chlorinated Solvents and Other DNAPLs in Ground Water, Waterloo Press, Portland, Oregon, 1996, p. 102.

3. B.H. Kueper and D.B. McWhorter, The behavior of dense, nonaqueous phase liquids in fractured clay and rock, Ground Water, 29:5 (1991) 716-728.

4. J.L. Wilson, S.H. Conrad, W.R. Mason, W. Peplinski, and E. Hagen, Laboratory Investigation of Residual Liquid Organics, USEPA/600/6-90/004, Robert S. Kerr Environmental Research Laboratory, Ada, Oklahoma, 1990.

5. F.A.L. Dullien, Porous Media Fluid Transport and Pore Structure, Academic Press, Inc., New York, New York, 1979.

6. M.K. Hubbert, Entrapment of petroleum under hydrodynamic conditions, Bulletin of the American Association of Petroleum Geologists, 37:8 (1953) 1954-2026.

7. R.D. Holtz and W.D. Kovacs, An Introduction to Geotechnical Engineering, Prentice Hall, Englewood Cliffs, NJ, 1981, p. 175.